Deciphering the regulon of the *Streptomyces coelicolor* AbrC3, a positive response regulator of antibiotic production.

Running tittle: AbrC3 regulon of *Streptomyces coelicolor*

Sergio Rico[1], Ramón I. Santamaría[1], Ana Yepes[2], Héctor Rodríguez[1], Emma Laing[3], Giselda Bucca[3], Colin P. Smith[3] and Margarita Díaz[1#]

[1]Instituto de Biología Funcional y Genómica (IBFG)/Departamento de Microbiología y Genética. Consejo Superior de Investigaciones Científicas (CSIC)/Universidad de Salamanca, Salamanca, Spain

[2] Institute for Molecular Infection Biology (IMIB). Julius-Maximilians-Universität Würzburg. Würzburg, Germany.

[3]Department of Microbial and Cellular Sciences, Faculty of Health and Medical Sciences, University of Surrey, Guildford, Surrey, UK.

[#] Address correspondence to Margarita Díaz, mardi@usal.es

ABSTRACT

The atypical two-component system (TCS) AbrC1/2/3 (encoded respectively by *SCO4598/4597/4596*), comprising two histidine kinases (HKs) and a response regulator (RR), is crucial for antibiotic production in *Streptomyces coelicolor* and for morphological differentiation under certain nutritional conditions. In this study we demonstrate that deletion of the RR-encoding gene *abrC3*, *SCO4596*, results in a dramatic decrease in ACT and RED production and delays morphological development. In contrast, the over-expression of *abrC3* in the parent strain leads to a 33% increase in ACT production in liquid medium. Transcriptomic and ChIP-chip analyses of Δ*abrC3* and the parent strain revealed that AbrC3 directly controls ACT production by binding to the *actII-ORF4* promoter region; this was independently verified by *in vitro* DNA-binding assays. This binding is dependent on the sequence (5'-GAASGSGRMS-3'). In contrast, the regulation of RED production is not due to direct binding of AbrC3, either to the *redZ* or to the *redD* promoters regions. This study also revealed other members of the AbrC3 regulon: AbrC3 is a positive autoregulator, which also binds to the promoter regions of *SCO0736*, *bdtA* (*SCO3328*), *absR1* (*SCO6992*), and *SCO6809.* The direct targets share the ten-base consensus binding sequence and may be responsible for some of the phenotypes of the Δ*abrC3* mutant. The identification of the AbrC3 regulon as part of the complex regulatory network governing antibiotic production widens our knowledge regarding TCS involvement in control of antibiotic synthesis and may contribute to the rational design of new hyper-producer host strains through genetic manipulation of such systems.

INTRODUCTION

Antibiotic production in *Streptomyces* is a complex process controlled by multiple factors through intricate genetic networks (1-4). This organism inhabits the soil where the environmental conditions are extremely variable and it must therefore compete with other organisms for scarce nutrients. Secretion of antibiotics provides a selective advantage to survive in this adverse environment (5) where it is important to respond quickly to different stimuli.

TCSs are perhaps the most important signal transduction mechanism in bacteria (Mist-web: http://mistdb.com/; P2CS-web: http://www.p2cs.org/index.php?PHPSESSID=4c2f13770410fa0fab046d10e6cf90d1) (6, 7). Their relative abundance in a genome reflects an organism's ability to adapt to different conditions, being less abundant for example in pathogens such as *Chlamydia* and *Rickettsia* than in free-living organisms such as *Streptomyces* or *Myxococcus* where more than 60 TCSs are present in their respective genomes (8-10). The only bacterial species lacking TCSs are intracellular pathogens (e.g. *Mycoplasma* species) and endosymbionts (e.g. *Amoebophilus* species) with severely reduced genomes (11).

The *Streptomyces* AbrC1/2/3 gene cluster (*SCO4598/97/96*) constitutes an atypical TCS in that it consists of two histidine kinases (AbrC1 and AbrC2 HKs) of group II and one response regulator (AbrC3 RR) belonging to NarL group of the HTH LuxR family regulators (12). It is conserved across all *Streptomyces* species sequenced to date and is found to be critical for antibiotic production and morphological differentiation under certain culture conditions in *S. coelicolor* (13). Both kinases of the system (AbrC1 and AbrC2) share high similarity in their kinase domains (85%) although AbrC1 lacks an internal domain of 50 amino acid residues of AbrC2. Independent promoters control these three genes, even though the genes for HKs and cognate RRs of TCSs are usually

arranged in operons (14); these features are conserved in all sequenced *Streptomyces* species, suggesting the importance for regulation of these genes. The RR, AbrC3, has orthologues in more than 20 *Streptomyces* species sequenced, sharing more than 90% amino acid identity among them. The deletion of these three genes correlates with delayed morphological differentiation and a marked reduction in the production of the antibiotics in *S. coelicolor* M145: actinorhodin (ACT), undecylprodiginine (RED) and the calcium-dependent antibiotic (CDA) (13).

In this work we present a detailed genetic, physiological and biochemical characterization of this important regulatory system. We show that deletion of *abrC3* alone leads to a dramatic reduction in ACT and RED production and morphological development in *S. coelicolor*. Moreover, overexpression of the AbrC3 regulator yields to high ACT production both in *S. coelicolor* and *S. lividans*. To better characterize the pleiotropic effects exhibited by Δ*abrC3,* we conducted a global transcriptome analysis comparing the Δ*abrC3* and the parental strain and show that the low production of ACT observed in the *abrC3* mutant is due to a general down-regulation of transcription of the *act* gene cluster. Other regulatory genes previously associated with antibiotic production, such as *sihf* (*SCO1480*) (15, 16), *afsS* (*SCO4425*) (17, 18) and *absR1* (*SCO6992*) (19), and with morphological development, for example, *wblE* (*SCO5240*) (20, 21) and *bdtA* (*SCO3328*) (22, 23) are also down-regulated in this mutant. Furthermore, through ChIP-chip analyses, we demonstrate a direct regulation of *act* gene expression through AbrC3 and provide independent verification with *in vitro* DNA-binding studies. This genome-wide study also revealed additional direct DNA targets of AbrC3. All of these targets share a common 10 bp sequence (5'-GAASGSGRMS-3') (S: G or C; R: A or G; M: A or C) and we have shown, by mutagenesis, that it is indispensable for the binding of AbrC3 to the *actII-ORF4*

promoter region. Therefore this sequence defines the putative consensus AbrC3 binding site.

MATERIALS AND METHODS

Strains, media and culture conditions

Escherichia coli strain BW25113(pIJ790) (containing the λRed system) is an *E. coli* K12 (*ΔaraBAD, ΔrhaBAD)* derivative (24) and non-methylating ET12567(pUZ8002) is a *dam, dcm, hsdS, cat, tet* strain harbouring the *tra* genes in the non-transmissible RP4-derivative plasmid, pUZ8002 (25). Both strains were grown in Luria–Bertani (LB) liquid broth or on LB agar (26). For CDA bioassays a parent strain of *Bacillus subtilis* (CECT 4522) was grown as an overlay on NA medium (27). *S. lividans* 66, *S. coelicolor* M145 (prototroph, $SCP1^{-}$, $SCP2^{-}$) and mutant strains were grown on R2YE and MS solid media for transformation and sporulation respectively (28). The liquid cultures used for transcriptional profiling and ChIP-chip were grown in NB medium at 30 ºC in 500 ml baffled flasks with 160 ml of medium each in a shaking orbital incubator (250 rpm). When necessary the media was supplemented with antibiotics (*E. coli* media: 100 μg ml^{-1} for ampicillin, 50 μg ml^{-1} for apramycin, 50 μg ml^{-1} for kanamycin, 34 μg ml^{-1} for chloramphenicol, and 25 μg ml^{-1} for nalidixic acid. *S. coelicolor* media: 20 μg ml^{-1} for neomycin, 50 μg ml^{-1} for apramycin, and 20 μg ml^{-1} for hygromycin).

Nucleic acid manipulations

Plasmid isolation, restriction enzyme digestion, ligation, and transformation of *E. coli* and *S. coelicolor* were carried out as described in Sambrook *et al* (26) and Kieser *et al*

(28), respectively. The plasmids and cosmids used are listed in Table S1. Total genomic DNA from *S. coelicolor* (gDNA) was isolated from a 24-36 h cultures in TSB medium following the procedure described in Hopwood *et al* (27), but scaled to 1-2 g of mycelium.

When needed the DNA was sequenced on both strands using a Perkin Elmer ABI Prism 377 DNA sequencer. *In silico* plasmid designs were obtained with the Gene Construction Kit software (GCK, Texco).

Plasmid constructions

Integrative plasmid pSETabrC3 was constructed by cloning the *abrC3* gene under the regulation of its own promoter into the shuttle *Streptomyces* integrative plasmid pSET152.Tio using NdeI and BamHI restriction sites. This plasmid was used for complementation of the Δ*abrC3* mutant strain (Table S1).

The low copy number pHJLAbrC3 plasmid derived from pHJL401 (29) was obtained by cloning the *abrC3* gene with its own promoter into pHJL401 using BamHI/EcoRI sites.

The new plasmids were introduced into the corresponding *Streptomyces* strains by protoplast transformation as previously described (28).

E. coli expression vector pETabrC3 was a derivative of pET22(b) plasmid, obtained by cloning the coding sequence for AbrC3 previously amplified by PCR with the corresponding oligonucleotides SRG-001 and SRG-002 (Table S2) in the NdeI/XhoI sites of the polylinker.

AbrC3 over-expression in *E. coli*

Cultures of *E.coli* BL21(DE3) transformed with pETabrC3 were induced with 1 mM IPTG to overproduce the AbrC3x6-His, subsequently purified with Ni-NTA (Qiagen) as

described before (30) and used to immunise two rabbits in order to obtain anti-AbrC3 antibodies.

Mutant construction (*abrC3* knockout)

The PCR-targeted system established by Gust *et al.* (31), was used to replace the complete coding sequence of *abrC3* (*SCO4596*) located in cosmid SCD20 (http://streptomyces.org.uk/) by the apramycin resistant gene *aac(3)IV*. The primers used to amplify the mutagenic cassette with pIJ773 as a template are listed in Table S2. The mutated cosmid SCD20Δ*abrC3::acc(3)IV* obtained in *E. coli* BW25113(pIJ790) was demethylated in *E. coli* ET12567(pUZ8002) and transferred by conjugation to *S. coelicolor* M145. The desired double recombinants carrying apramycin resistance, while being sensitive to kanamycin (the selection marker for the vector sequences), were selected. Southern blotting and PCR assays confirmed the deletion of the *abrC3* gene in *S. coelicolor* M145.

RNA isolation and DNA microarrays analysis

For RNA extraction from *S. coelicolor* parent strain and Δ*abrC3* mutant strains, 160 mL of NB media was inoculated in 500 mL baffled flasks with 4 x 10^6 spores/mL and incubated at 30 ºC for 36, 48, and 60 h. Two biological replicates and three technical replicates were used for each time-point. Prior to RNA isolation using a modified version of mirVana miRNA Isolation kit protocol (Life Technologies), cells from 20 mL of culture were harvested and suspended in RNA-protect Bacteria Reagent (Qiagen). Following mycelial lysis with lysozyme (15 mg/ml in TE at room temperature), three vol. of RLT buffer from the RNeasy mini plus kit (Qiagen) were added and mycelia were disrupted using a TissueLyser (Qiagen) for 4 min. The lysate was clarified by centrifugation, extracted twice with phenol/chroroform and once with

chloroform and applied to a gDNA eliminator filter (RNeasy mini Plus, Qiagen) to remove any contaminating DNA. After this step 1.25 vol of 100 % ethanol were added and the total RNAs (including small RNAs) were purified through the mirVANA columns following the manufacturer's recommendations. The quality and concentration of RNA were assayed using the Bioanalyzer 2100 system and spectrophotometric assays (Agilent and Nanodrop ND1000, respectively).

The *S. coelicolor* IJISS 105K microarray used for ChIP-chip and high-resolution transcriptome analysis, was designed by the Functional Genomics Laboratory of Surrey University (UK) in collaboration with Oxford Gene Technology (UK), and manufactured by Agilent. They comprise almost 105,000 unique 60-mers with an average genome spacing of 35 nucleotides. The 105K probes are designed to cover the coding strands of all known protein coding genes and both strands of all intergenic regions. A cDNA *versus* reference gDNA microarray two-colour experimental design was utilised for the transcriptomic comparison *of S. coelicolor* M145 and Δ*abrC3*. All Cy3-cDNA and Cy5-gDNA labelling reactions and hybridisation assays were performed according to the recommendations described in http://www.surrey.ac.uk/fhms/microarrays/Downloads/Protocols/index.htm

All hybridised arrays (expression and ChIP-chip) were scanned using an Agilent Technologies microarray scanner and resultant images were analysed using Agilent Technologies Feature Extraction software (version 9.1.3.1.) with local background correction.

Raw gene expression data were normalised within the statistical computing environment R using the LIMMA package (32-34) global median within-array normalization, followed by the 'scale' across-array normalization was applied. Probes that were flagged as poor quality by Agilent Feature Extraction were removed from the

188 analysis. A gene's expression was calculated by averaging across all remaining good
189 quality probes that target the annotated coding sequence. Expression data sets were
190 analysed using rank products analysis via RankProdIt (http://strep-
191 microarray.sbs.surrey.ac.uk/RankProducts), a web-interactive analysis tool (35).
192 Differentially expressed genes were identified as having a *pfp* (*p*robability of *f*als*e*
193 *p*rediction) value less than or equal to 0.15, equal to a false discovery rate of
194 approximately 15 % and at a level that has been experimentally validated (in this study)
195 and others (e.g. (36). A BED formatted track with the average Log_2 expression data to
196 be visualised across the chromosome using the UCSC microbial gene browser
197 (http://microbes.ucsc.edu/) was generated using in-house Perl scripts. All data are
198 MIAME compliant and the raw and normalized data have been deposited in
199 ArrayExpress (accession number E-MTAB-1453).
200
201 **qRT-PCR**

202 Real-time quantitative RT-PCR (qRT-PCR) was used to validate the microarray data.
203 Specific primers and probes for the tested genes were designed using the Primer3 web-
204 based tool (Table S2). Five-µg RNA samples were treated with RNAase-free DNaseI
205 (Promega) according to the manufacturer instructions. One µg of the resulting RNA was
206 used as template for cDNA synthesis using iScript Reverse Transcription Supermix for
207 RT-qPCR (Bio-Rad) in 20 μl reaction volumes. The samples were diluted 1:1 with
208 distilled water and 5 μl was used in the quantitative PCR reaction with 10 pmol of
209 forward and reverse primer, 2.5 pmol of FAM/TAMRA dual-labelled specific probe,
210 and 12.5 μl SsoFast™ Probes Supermix with ROX master mix (Bio-Rad) in a final
211 volume of 25 μl. Each assay was performed in duplicate using CFX96 Touch™ Real-

Time PCR Detection System (Bio-Rad). Control PCRs were included to verify that there was no DNA contamination (without RT, enzyme negative control). Relative quantification of gene expression was performed by the ΔΔCt method, a comparative qPCR data analysis (37) in which, the Ct values of the genes of interest obtained from two different experimental RNA samples (parent strain and mutant) are directly normalized to the Ct values of a housekeeping gene (gene control) in the same samples. First, the difference between the Ct values of the gene of interest between parent and mutant strains (ΔCt^1) and difference of Ct values of the housekeeping gene between both strains (ΔCt^2) are calculated for each experimental sample. Then, the difference in the ΔCt values between the gene of interest and control gene (ΔCt^1-ΔCt^2 = ΔΔCt) is calculated. The fold-change in expression of the gene of interest between the two experimental samples (parent strain and mutant) is then equal to $2^{-\Delta\Delta Ct}$. The gene *hrdB* (*SCO5820*) was the internal control used to quantify the relative expression of the target genes, since its expression level remained constant in all the conditions analyzed by microarray. The expression ratios measured by microarrays and by qRT-PCR assay were plotted, and the linear correlation coefficient was calculated ($y = 1.60x – 0,09$; $R^2 = 0.93$) (Table 3).

ChIP-chip analysis

For Chromatin Inmunoprecipitation (IP) three aliquots of 20 mL from the same cultures used in the microarray gene expression analysis were taken (*S. coelicolor* M145 and Δ*abrC3* mutant strains incubated at 30 ºC for 36, 48, and 60 h). These samples were treated with formaldehyde (Sigma) at a final concentration of 1 %. Crosslinking was allowed to proceed for 30 min at 30 ºC. Glycine, at a final concentration of 0.5 M was added to stop the crosslinking for a further 5 min at 30 ºC. Mycelium was harvested by

centrifugation and frozen at -20 ºC. Chromatin of average size range 300-600 bp was obtained as described in Bucca et al (38). Chromatin IP was carried out as described before (38) using purified rabbit polyclonal antibodies against AbrC3 obtained in our laboratory. The IgG fraction containing anti-AbrC3 polyclonal antibodies and the fraction from preimmune serum from the same rabbit used for immunisation was purified by affinity chromatography using CNBr activated Sepharose 4B (Sigma). The chromatin purified from *S. coelicolor* M145 and Δ*abrC3* mutant strains was sonicated to obtain an average size range of 300-600 bp. DNA samples were immunoprecipitated with either AbrC3 antibodies (abIP) or mock control (NoIP), purified, labelled with Cy3 or Cy5-dCTP respectively and hybridized to 105K arrays as described above. Two biological replicates were hybridized such that the AbIP/NoIP samples from each of the two replicates were labeled in opposite dye orientations to control for dye bias. Arrays were scanned and processed as described above.

The raw data were normalized within R (as above) using the across-array scale function of the LIMMA package only. Again, poor quality probes were filtered out from downstream analysis. The data analysis was carried out essentially as described by Allenby *et al.* (39). Significant probes ($p < 0.05$) defined on the basis of a non-parametric t-test run with 'multtest' and 'pnorm' (within R) were plotted as ratio of [(parent strain Ab IP/mock IP) / (Δ*abrC3* Ab IP/mock IP)]. The probes most differentially-enriched for AbrC3 binding between the parent strain and the mutant were selected from the right tail of the distribution. Probes within 3 kb (based on their annotated genomic location) of each other were 'grouped' and genomic regions of interest were those in which at least two enriched probes were found. Finally, tracks (BED files) to visualise the data across the chromosome using the UCSC microbial genome browser (http://microbes.ucsc.edu/) were generated using in-house Perl scripts.

The raw and normalized ChIP-chip data have been deposited in ArrayExpress (accession number E-MTAB-1451).

Western blot assays

Total protein extracts were obtained from 5 mL samples (in triplicate) of the cultures used for the global analysis described above. The proteins were resolved in SDS-PAGE (15 % polyacrylamide in a MiniProtean II system, BioRad). After transfer to Inmobilon-P (Millipore) the proteins were reacted with pre purified polyclonal 1:100000 dilution of anti-AbrC3. AbrC3 was detected by chemiluminescence with ECL western blotting detection reagents following the manufacturer's instructions (GE Healthcare) using horseradish peroxidase-coupled anti-rabbit secondary antibody.

***In vitro* DNA-binding assays**

Gel-shift assays were conducted using DNA fragments containing the intergenic region (up to -400 bp from the translational start point) plus 100 (+ 100 inside the ORF) were amplified using the corresponding primers in a PCR reaction (Table S2). These fragments were 5'-radiolabelled with T4 polynucleotide kinase in the presence of [γ-^{32}P]-dATP, and the unreacted [γ-^{32}P]-dATP was removed using Illustra ProbeQuant TM G-50 Micro Columns (GE HealthCare, USA). The purified proteins were incubated in Tris-HCl 50 mM pH 7, $MgCl_2$ 25 mM, NaCl 0.1 M at 30 ºC for 30 min, prior to the binding. Then, different concentrations of the proteins were incubated with the labelled DNA probes (10 fmol) in binding buffer (Tris-HCl 10 mM pH 7.8, DTT 2 mM, NaCl 150 mM, glycerol 10 % and 45 ng of sheared salmon sperm DNA) for 30 min at 30 ºC. Protein bound DNA and free DNA were resolved on 5 % acrylamide gel in 0.5 X TBE buffer (Tris 44,5 mM, boric acid 44,5 mM, EDTA 1 mM pH 8) at 4º C. The gel was

exposed overnight and autoradiography revealed. As control, unlabelled specific probe (S) (100-fold molar excess) or non-specific competitor DNA (N) (100-fold molar excess of sheared salmon sperm DNA) were added to the reaction mixture. Also a BSA protein binding reaction (4 μM) was conducted as a control to demonstrate the specificity of the EMSAs.

Identification of the putative AbrC3 binding site

The Regulatory Sequence Analysis Tools (RSAT) "consensus" alignment (http://rsat.ulb.ac.be/) was used to identify putative DNA conserved sequences in the upstream regions (with respect to the annotated translation start codon) of the AbrC3 target genes (including 100 bp into the respective ORF), identified from the ChIP-chip experiment.

The functionality of the conserved ten-base sequence, identified with RSAT consensus alignment, was demonstrated by eliminating it from the *actII-ORF4p* p. The elimination of this sequence was achieved using overlapping PCR. As a first step, PCR amplicons were made using primers SRG95/SRG97 and SRG96/SRG90, respectively (Table S2). Using both resulting fragments as templates, a second PCR was conducted using oligonucleotides SRG95/SRG90. The final fragment, with EcoRI/PstI sites in the ends, was cloned into the pGEM T-easy plasmid. The elimination of the consensus binding sequence from the *absR1p* was performed by PCR amplification of the region with the oligonucleotides SRG-116/SRG073 (Table S2).

Antibiotic production measurements

Production of ACT in liquid cultures was determined measuring A_{640} (ε_{640}= 25320) in the supernatant of samples treated with 1N KOH overnight at 4 ºC and centrifuged

312 (15000 g, 10 min). The experiments were all performed in triplicate and the dry weight
313 of samples at different times was measured to monitor culture growth.

314 **Chromatographic analysis**

315 Liquid cultures were centrifuged and supernatants and cell pellets were extracted
316 separately. The supernatants were extracted twice with an equal volume of ethyl acetate
317 containing 1% formic acid. The cell pellets were extracted with acetonitrile. In each
318 case, the solvent was evaporated and the residue re-dissolved in a small volume of a
319 mixture of dimethyl sulfoxide and methanol (50:50). These samples were
320 chromatographed as previously described (40).

321

322 **RESULTS**

323 **Influence of the AbrC3 RR in antibiotic production in *Streptomyces***

324 The *S. coelicolor* Δ*abrC3* mutant strain was generated using the PCR-targeting
325 approach described by Gust *et al.* (31), which replaced the entire coding region of the
326 gene with an apramycin resistance cassette (see Materials and Methods). Phenotypic
327 analysis of growth and antibiotic production of the parent strain (M145 strain), Δ*abrC3*
328 and the triple mutant Δ*abrC1/C2/C3*, previously described (13), revealed significant
329 differences among the three strains (Figure 1A). ACT and RED production were highly
330 diminished in both the triple and single mutant compared to the parent strain on nutrient
331 agar medium. In contrast, CDA production in the mutant lacking only the response
332 regulator, Δ*abrC3*, was unaffected while it was clearly diminished in the triple mutant.
333 A delay in morphological differentiation on solid medium was also observed in both
334 mutants. When the strains were grown in liquid nutrient broth (NB) the Δ*abrC3* mutant

produced almost no ACT. Complementation of the Δ*abrC3* mutant with the integrative plasmid pSET152-abrC3 restored ACT production to almost parent strain levels (Figure 1B). Both mutants and the parent strain produced similar growth curves (e.g., Figure S1A) indicating that growth *per se* was not compromised in the mutant strains.

Complementation with pSET152-abrC3 was also tested on solid medium (NA). ACT production and morphological differentiation were complemented and there was a partial complementation of RED production (Figure 1B). It was noted that ACT production on solid medium was found to be higher in the complemented strain than in the parent strain harbouring the empty plasmid; pSET152-derivates tend to exist as tandem duplications in the genome (CPS, unpublished data) and it is therefore conceivable that an enhanced level of AbrC3 is responsible for the elevated ACT production.

It is noteworthy to mention that quantification of ACT production from M145 cells transformed with *abrC3* moderately overexpressed from the low copy number plasmid, pHJLabrC3 plasmid, showed 33% more ACT production at five days compared to the plasmid control, pHJL401 (Figure 2). This result was consistent with AbrC3 acting as a positive regulator of the ACT gene cluster and offers the possibility of using this low copy number plasmid to enhance antibiotic production. Indeed, when pHJLabrC3 was introduced into the *S. lividans 66* strain, the normally silent ACT pathway was induced to even higher levels than in *S. coelicolor* (Figure 2).

Effects of *abrC3* deletion on the *S. coelicolor* transcriptome

Comparison of genome-wide mRNA abundances between the parent strain *S. coelicolor* M145 and its congenic Δ*abrC3* mutant was performed. Samples from 36, 48, and 60 h growth (Figure S1-A) were taken and antibiotic production at these time points was

assessed by HPLC. As shown in Figure S1-B, at 60 h growth there was an ACT production peak in the parent strain but not in the mutant strain, in both the supernatant and cell extract fractions. Likewise, RED production was only observed in parent strain cell extracts. In addition, the level of AbrC3 protein in the parent strain and its absence in the mutant Δ*abrC3* strain at the three sampling points used in this study was confirmed by Western blotting using anti-AbrC3 antibodies (Figure S1-C).

Total RNA samples from the Δ*abrC3* mutant and the parent strain cultivated at 36, 48, and 60 h in NB medium were labelled and hybridized to 105K × 60-mer high density whole genome *S. coelicolor* IJSS DNA microarrays as described by Lewis *et al*. (41) (see Materials and Methods). Analysis of the DNA microarray data from two independent experiments revealed that only 32 genes were down-regulated and eight genes were up-regulated at a statistically significant level (Benjamini and Hochberg corrected *p*-values <0.005 and *pfp* <0.15 (*pfp*: *p*robability of *f*alse *p*rediction)) (see Tables 1 and 2). Of the 33 genes that showed a significantly reduced expression in the mutant strain, 16 corresponded to the entire *act* cluster, including *actII-ORF4* (*SCO5085*), which encodes the SARP pathway-specific regulator of the *act* cluster (Table 1). Three other significantly down-regulated genes encode regulatory proteins and were previously related to antibiotic regulation, *sIHF* (*SCO1480*) (15, 16), *afsS* (*SCO4425*) (17, 18), and *absR1* (*SCO6992*) (19). An additional gene encoding a putative transcriptional regulator with a helix-turn-helix motif, *SCO1839,* and two genes involved in morphological development, *wblE* (*SCO5240*, encoding an extra-cytoplasmic function sigma factor (20, 21)) and *bdtA* (*SCO3328*, encoding a putative transcription factor regulated by BldD, and that forms an operon with *SCO3327* (22, 23)) were also significantly down-regulated. The *acdH* gene (*SCO2779*) encoding an acyl-CoA dehydrogenase involved in branched amino acid catabolism in *S. coelicolor*

385 and *S. avermitilis* (42) and *SCO3218*, a gene of unknown function located in the *cda*
386 gene cluster, were also significantly down-regulated in the mutant (Table 1). Among the
387 eight genes significantly up-regulated were the ribosomal protein gene, *rplP* (*SCO4709*)
388 and *chpE* (*SCO1800*) (43) (see Table 2).
389 Several of the differentially expressed genes were selected for independent validation
390 by quantitative real time PCR (qRT-PCR) (Table 3). These included down regulated
391 genes: *acdH* (*SCO2779*) acyl-CoA dehydrogenase, *absR1* (*SCO6992*) activator of
392 secondary metabolism, a sigma-like protein gene *afsS* (*SCO4425*), and the specific
393 regulator of the ACT cluster, *actII-ORF4* (*SCO5085*). We also analyzed the expression
394 levels of one of the genes differentially up-regulated in the mutant that encodes the 50S
395 ribosomal protein L16 *rplP* (*SCO4709*). Moreover, we included both histidine kinase
396 genes of the TCS, *abrC1* and *abrC2* (*SCO4598* and *SCO4597*), in order to confirm their
397 non-differential expression levels. A good correlation of transcript measurements from
398 the microarray data and the qRT-PCR data (yielding a correlation regression coefficient
399 of 0.93) was obtained (Table 3). Note that the validation of differential expression for
400 *SCO4709* confirms the use of 0.15 as a suitable *pfp* threshold for determining
401 significance, similar to that found in other expression based studies (e.g. (36)).
402
403 ***In vivo* identification of AbrC3 targets on the *S. coelicolor* genome**
404 The genes exhibiting a marked AbrC3-dependent change in expression could be directly
405 regulated by AbrC3 or could be regulated by transcription factors downstream of AbrC3
406 in a possible regulatory cascade. Hence, to identify genes directly regulated by AbrC3,
407 by interaction with their respective promoter regions, a genome-wide ChIP-chip
408 approach was undertaken. Samples from the same cultures and time-points used for the
409 transcriptomic analysis (above), were treated with formaldehyde to cross-link proteins

410 to DNA and subjected to chromatin immunoprecipitation with either purified anti-
411 AbrC3 antibodies or mock controls (see Materials and Methods). The
412 immunoprecipitated DNA from each strain was labelled with Cy3 or Cy5 in a dye-
413 balanced direct comparison experimental design and hybridized to the above mentioned
414 105K *S. coelicolor* microarrays (see Materials and Methods). Two biological replicate
415 experiments were conducted and significantly enriched genomic binding regions in the
416 parent strain relative to the Δ*abrC3* mutant were identified. We identified 617, 520, and
417 458 AbrC-enriched (AbrC3 DNA targets bound at significant higher levels when
418 comparing parent strain to the mutant) regions from chromatin isolated at 36 h, 48 h,
419 and 60 h of growth, respectively. The genes with higher enrichment ratio are
420 summarized in Table 4 and the overlapping targets in ChIP-chip and transcriptome
421 analyses in Table 5.
422 This analysis demonstrates that the AbrC3 protein is able to bind *in vivo* to the promoter
423 of the pathway-specific regulator gene of the ACT cluster, *actII-ORF4p,* (*SCO5085*)
424 (Table 4 and 5) at 36 h with high efficiency. No binding was detectable at 48 h or 60 h.
425 This result suggests that the down-regulation of the *act* gene cluster (Table 1) is due to
426 the direct regulation of *actII-ORF4* exerted by AbrC3 at around 36 h culture time.
427 Efficient binding of AbrC3 to its own promoter *abrC3p* (*SCO4596*) at 60 h was also
428 observed (Table 5), indicating that AbrC3 is an autoregulator. No binding to the
429 promoters of the histidine kinase-encoding genes of the AbrC system (*abrC1* and
430 *abrC2*), nor differential expression of these two genes under the experimental
431 conditions used, was observed (Table 3).
432 *In vivo* binding of AbrC3 to several of the promoters of the genes previously identified
433 as down-regulated was observed and therefore their expression is very likely to be
434 directly controlled by AbrC3 (Table 5). Weaker AbrC3-enrichment was observed

435 upstream of genes *SCO1480* (sIHF), *SCO1550*, the regulator *SCO1839,* the acyl-CoA
436 dehydrogenase AcdH (*SCO2779*), and the transcription factor WblE (*SCO5240*), and no
437 binding at all was observed for three of the differentially expressed genes identified in
438 our transcriptome analysis: *SCO0682, SCO3218,* and *afsS* (*SCO4425*) (data not shown).
439 We hypothesize that these genes could be regulated by factors downstream of AbrC3 in
440 a possible regulatory cascade, or additional transcription factors/co-factors bound to the
441 promoter regions blocked access of the anti-AbrC3 antibody, yielding false negatives
442 (see, for example, (39)).
443 Among the significantly up-regulated genes, we could only detect binding of AbrC3 to
444 the putative promoters of the *rplP* (*SCO4709*) and *SCO6809* genes (Table 5),
445 suggesting that the other six up-regulated genes may be regulated by factors
446 downstream.
447 Electrophoretic mobility shift assays (EMSAs) were conducted to test the *in vitro*
448 binding capacity of the protein to the DNA sequences upstream of the corresponding
449 genes that showed AbrC3-binding *in vivo*. DNA fragments comprising intergenic region
450 (up to -400 bp from translation start point) plus 100 bp inside the ORF (+100) were
451 used to perform the experiments and were so on called promoters* (*SCOXXXXp*). Most
452 of the identified targets that were bound *in vivo* by the AbrC3 protein (Table 5) were
453 also able to be bound *in vitro* with high specificity: *actII-ORF4p*, *abrC3p, SCO0736p*,
454 *absR1p*, and *SCO6809p* (Figure 3A, 3B, 3C, 3D and 3H). The promoters* of *SCO2113*
455 and *bdtA* were bound with less specificity (Figure 3E and 3F) and some putative
456 promoters*, such as *SCO4709p,* did not yield mobility shifts *in vitro* (Figure 3G).
457 Competition experiments to verify the specificity of AbrC3 binding, to each promoter*,
458 were conducted by adding different amounts of the corresponding unlabelled DNA or
459 different amounts of sheared salmon sperm DNA to the binding reaction.

460

461 **Identification of a putative consensus AbrC3 binding site**

462 Aligning the 500 bp upstream sequences (including the first 100 bp of the respective
463 ORFs) of genes enriched for AbrC3 in the ChIP-chip and EMSA analyses using the
464 Regulatory Sequence Analysis Tools consensus alignment (http://rsat.ulb.ac.be/)
465 identified a minimal consensus-binding site for AbrC3. A common 10 bp sequence (5'-
466 GAASGSGRMS-3') was present in all of the putative promoters of the identified target
467 genes and was absent in the ones that did not yield mobility shifts *in vitro*, such as
468 *SCO4709p* (Figure 4A). This putative AbrC3-binding sequence was present within the
469 ORF of *actII-ORF4*, in the positions +72/+81 (from the translation start codon), near
470 one of the described target sequences of the regulator AtrA (44) (Figure 5). This
471 sequence was also found in 23 out of 30 of the genes identified by ChIP-chip (Table 4).
472 The functionality of this putative AbrC3-binding sequence was demonstrated by
473 EMSAs using different fragments of the *actII-ORF4p* or deleting the putative binding
474 sequence (Figure 4B). Only the whole promoter* region (fragment 1 used also in Figure
475 3), or a 3′ part of the promoter* that included the ten-base sequence generated a
476 mobility shift in the presence of the AbrC3 protein (Figures, 4B panels 1 and 4).
477 Conversely, the mobility shift did not take place when the ten-base sequence was
478 removed (see Materials and Methods) (Figure 4B panel 5); controls used to demonstrate
479 the specificity of AbrC3-binding to the 3′ segment of the promoter* (fragment 4) are
480 shown in Figure 4C. This result clearly indicated that the sequence (5'-
481 GAAGGCGACC-3') was essential in the direct regulation of the *actII-ORF4* expression
482 by the AbrC3 regulator.

483 The importance of this sequence in the binding of AbrC3 was also demonstrated by
484 EMSA with *absR1p*, another direct target of this regulator. The elimination of the

485 proposed binding-sequence (5'-GAAGGGGACG-3') originated the sequence
486 *absR1pDel* unable to bind AbrC3, and therefore the shifted band was not observed.
487 (Figure S2).

488 Moreover, EMSAs were performed using shorter DNA probes consisting in a 50 bp
489 labeled oligonucleotide (resulted from annealing two complementary long
490 oligonucleotides SRG119/120 (Table S2)) corresponding to a small fragment from
491 *actIIORF4p* and containing the predicted binding sequence (probe 1) and also another
492 artificial labeled oligonucleotide with the same size containing this sequence but
493 surrounded by foreign DNA (probe 2: annealing of oligonucleotides SRG121/122
494 (Table S2)). The results (Figure S3) showed the ability of AbrC3 to bind specifically to
495 probe 1 and also to the artificial probe 2. Therefore these 10 nucleotides (5'-
496 GAAGGCGACC-3') were enough to recruit the protein.

497 **DISCUSSION**

498 **AbrC3 directly regulates *actII-ORF4* expression**

499 An integrated global ChIP-chip and transcriptome analysis of parent strain *S. coelicolor*
500 and an *abrC3* mutant derivative has identified the regulon of the response regulator
501 AbrC3. *actII-ORF4*, the pathway-specific regulator of ACT, is one of its direct targets
502 as corroborated by EMSA *in vitro*. A 10 bp sequence, 5'-GAASGSGRMS-3', identified
503 by RSAT consensus alignment of the putative promoters* targeted by AbrC3 defines
504 the AbrC3 binding site. In the case of *actII-ORF4*, the binding sequence (5'-
505 GAAGGCGACC-3') is found within the ORF at the position +72/+81 (from the
506 translational starting ATG) (Figure 5). It is not the first time that a transcriptional
507 regulator-binding site is found within the *actII-ORF4* coding sequence; there are two
508 other regulators, AtrA and Crp, whose binding sites are in position +45/+69 (44) and

509 +24/+38 (45), respectively. DNase footprinting assays using selected AbrC3 associated
510 sequences failed to yield a DNase-protected region (data not shown); we consider that
511 the observed poor solubility of AbrC3 *in vitro* may account for the incomplete shifting
512 of template DNA obtained in the EMSAs and for our failure to observe a footprint.
513 Nevertheless, this consensus sequence has been shown indispensable for AbrC3 binding
514 to the *actII-ORF4*p (Figure 4) and for another of its targets (*absR1p*) (Figure S2). We
515 speculate that binding of AbrC3 to the *actII-ORF4p* at 36 h may be necessary for the
516 recruitment of other regulators and that the binding of these is necessary for the first
517 steps of *actII-ORF4* expression: after this initial 'recruitment' the regulators are
518 subsequently released from the promoter* to allow expression of downstream genes.

519 The expression of the ACT-specific pathway regulator *actII-ORF4* is under the control
520 of different regulatory proteins that respond to diverse signaling routes in *S. coelicolor*
521 such as PhoP/R (46) and RapA1/A2 (47), LAL regulators SCO0877 and SCO7173 (48),
522 ECF SigT (49), among others (reviewed by van Wezel and McDowall (3)). To date,
523 demonstration of the direct binding of transcription factors to the *actII-ORF4* promoter
524 region is limited (Figure 5). *In vitro* binding assays (EMSAs) have shown that the AtrA
525 protein binds to the *actII-ORF4* promoter (44). More recently, DNA affinity capture
526 assays have shown the capability of four more proteins (SCO0310, SCO3932,
527 SCO5405 and AdpA) to bind to the *actII-ORF4* promoter (15). Among the TCSs
528 implicated in antibiotic production only AbsA2 has, thus far, been shown to bind to the
529 *actII-ORF4* promoter *in vivo* (50). Very recently, EMSAs have demonstrated the *in*
530 *vitro* binding of the TCSs DraR/K and AfsQ1/Q2 to the *actII-ORF4* promoter (51, 52).
531 Control of secondary metabolism by the global regulator Crp has also recently been
532 described and Crp binding to *actII-ORF4* detected by ChIP-chip, being both of the two

binding sites described within the ORF, in positions +24/+38 and +234/+248 (Figure 5) (45).

AbrC3 regulon

The putative binding sequence (5'-GAASGSGRMS-3') defined in this work is present in 23 out of 30 genes with the highest binding enrichment (WT AbIP/NoAbIP vs Δ*abrC3* AbIP/NoAbIP enrichment ratio obtained in the ChIP-chip assay) (Table 4). The position of the putative binding sequence is typically upstream of the respective ORF suggesting regulation of the gene downstream of the binding site. However, in some cases the target sequences are within the coding sequences. This feature is coincident with data described previously in the study of the regulation exerted by the protein Crp where more than 50 % of all Crp-associated sequences were mapped within ORFs (45). The regulatory role of these sequences located inside the ORFs is not clear and in a recent study, using ChIP-seq and ChAP-seq technologies to characterize the AdpA regulon, it was found that approximately 75 % of the *in vivo* AdpA-binding sites apparently have no function in the regulation of gene expression (53).

Conversely, it is also possible that some *bona fide* AbrC3 targets were missed in this study because the antibody does not recognize the epitopes when AbrC3 is one of several transcription factors bound to the promoter regions. It is known that false negatives can occur in ChIP-chip studies (38).

Pleiotropic regulation by the *abrC* TCS

The pleiotropic phenotype of the triple Δ*abrC1/2/3* mutant (13) shows relative differences (decreased CDA production) when compared to the phenotype of the RR gene deletion mutant, Δ*abrC3*. This result suggests that other RRs may be controlled by the kinases of this TCS such as the orphan RR *SCO2281* proposed by Wang *et al* to be

558 recognized by AbrC2 (54). It is known that the biosynthetic RED genes are expressed
559 early, so the existence of AbrC3 direct regulation to the promoter regions of *redD* or
560 *redZ* cannot yet be excluded with the experimental conditions tested. If the RED cluster
561 regulation by AbrC3 is indirect, this could be exerted through the regulatory cascade
562 triggered by AfsS, that is one of the indirect AbrC3 targets (17, 18), or by sIHF, down-
563 regulated in Δ*abrC3* and able to bind to the *redD* and *redZ* promoters (15, 16).
564 Several transcriptional regulators, whose encoding genes were down-regulated in our
565 study could be responsible of the morphological phenotype observed in the *ΔabrC3*
566 mutant: sIHF that also binds to the *bldD* promoter, a key regulator of development in *S.*
567 *coelicolor* (16); the extracytoplasmic function sigma factor, WblE (20, 21); and BdtA a
568 putative transcription factor regulated by BldD involved in morphological
569 differentiation (22, 23).
570 ChIP-chip assays demonstrated that AbrC3 is an autoregulator. No differential
571 regulation between the wild type strain and the AbrC3 mutant of the two kinase-
572 encoding genes of the AbrC TCS system was identified in our ChIP-chip or
573 transcriptome analysis.
574 A summary of the main interactions within the AbrC3 regulon deduced from our global
575 *in vivo* analyses (ChIP-chip and transcriptome analysis) is illustrated in the model
576 depicted in Figure 6. We have observed a global positive effect on secondary
577 metabolism, mainly on the ACT cluster, and morphological differentiation through the
578 direct interaction of AbrC3 with the different genes mentioned above. This activation
579 could also be facilitated by a negative control of AbrC3 on primary metabolism through
580 ribosomal proteins such as RplP. Indeed, another gene involved in primary metabolism,
581 *acdH*, is down-regulated in the Δ*abrC3* mutant; this gene encodes an Acyl-CoA
582 dehydrogenase involved in biosynthesis of precursors of ACT and RED and that could

583 explain the positive regulation of this gene by AbrC3. Besides, Wang *et al*. have just
584 reported *in vitro* evidence that *abrC3* is a target of AfsQ1 and that it positively regulates
585 its expression. This suggests that the function of AfsQ1/Q2 is at least partly mediated
586 via the AbrC1/C2/C3 system, further illustrating the complexity of the regulatory
587 network governing antibiotic production (Figure 6) (51, 52).

588 The emergence of new antibiotic resistant isolates makes new antibiotic discovery and
589 the improvement of their production major challenges for microbial biotechnology.
590 Widening our knowledge regarding TCS involvement in antibiotic synthesis regulation
591 can contribute to the rational design of new hyper-producer host strains through genetic
592 manipulation of those complex systems. Moreover, strategies involving TCS could be
593 used to unveil new antimicrobial molecules that are not normally produced under
594 laboratory culture conditions.

595

596 **ACKNOWLEDGEMENTS**

597 Thanks are due to MJ Jiménez Rufo for her excellent technical work and to A. Braña for
598 his chromatographic analysis.

599 This work was supported by Spanish Comisión Interministerial de Ciencia y Tecnología
600 (CICYT) [GEN2003-20245-C09-02]; Junta de Castilla y León (JCyL) [SA072A07,
601 CSI099A12-1]; Spanish Ministerio de Ciencia e Innovación (MICINN) [BFU2010-
602 17551] and Fundación Ramón Areces institutional funding to the IBFG. S. R. had a
603 JAE-predoctoral grant from the CSIC. H.R. had a postdoctoral fellowship from Botín
604 Foundation.

605

606

607

608 **SUPPLEMENTARY DATA**

609 Figure S1: Phenotypic features of cultures used for ChIP-chip and transcriptome
610 analysis. A) Growth curves of parent strain M145 and Δ*abrC3* strains in NB medium at
611 30 ºC. The cultures times selected for RNA isolation are encircled. B) HPLC profiles of
612 60 h samples showing ACT and RED antibiotic production in M145 (black) and
613 Δ*abrC3* (grey) strains. C) Western blot of the samples selected (36, 48 and 60 hours) in
614 two biological duplicates using anti-AbrC3 antibodies.
615 Figure S2: EMSA of AbrC3 protein with *absR1p* and *absR1pDel* (the same region
616 without the putative proposed binding-sequence, 5'- GAAGGGGACG -3').
617 Figure S3: EMSA of AbrC3 protein with *actII-ORF4* 50-bp oligonucleotide containing
618 the proposed binding-sequence (5'-GAAGGCGACC-3') (Probe 1) and an artificial 50-
619 pb oligonucleotide including this sequence (5'-GAAGGCGACC-3') but surrounded by
620 foreign DNA (Probe 2).
621 Table S1: Plasmids and cosmids used in this work
622 Table S2: Oligonucleotides used in this work

623

REFERENCES

1. **Bibb M, Hesketh A.** 2009. Chapter 4. Analyzing the regulation of antibiotic production in streptomycetes. Methods Enzymol **458:**93-116.
2. **Huang J, Shi J, Molle V, Sohlberg B, Weaver D, Bibb MJ, Karoonuthaisiri N, Lih CJ, Kao CM, Buttner MJ, Cohen SN.** 2005. Cross-regulation among disparate antibiotic biosynthetic pathways of *Streptomyces coelicolor*. Mol Microbiol **58:**1276-1287.
3. **van Wezel GP, McDowall KJ.** 2011. The regulation of the secondary metabolism of *Streptomyces*: new links and experimental advances. Nat Prod Rep **28:**1311-1333.
4. **Liu G, Chater KF, Chandra G, Niu G, Tan H.** 2013. Molecular regulation of antibiotic biosynthesis in *Streptomyces*. Microbiol Mol Biol Rev **77:**112-143.
5. **Hopwood DA.** 2007. Streptomyces in nature and medicine. The antibiotic makers. Oxford University Press Inc, New York.
6. **Barakat M, Ortet P, Jourlin-Castelli C, Ansaldi M, Mejean V, Whitworth DE.** 2009. P2CS: a two-component system resource for prokaryotic signal transduction research. BMC Genomics **10:**315.
7. **Ulrich LE, Zhulin IB.** 2010. The MiST2 database: a comprehensive genomics resource on microbial signal transduction. Nucleic Acids Res **38:**D401-D407.
8. **Lee B, Schramm A, Jagadeesan S, Higgs PI.** 2010. Two-component systems and regulation of developmental progression in *Myxococcus xanthus*. Methods Enzymol **471:**253-278.
9. **Kim D, Forst S.** 2001. Genomic analysis of the histidine kinase family in bacteria and archaea. Microbiology **147:**1197-1212.

10. **Kim S, Hirakawa H, Muta S, Kuhara S.** 2010. Identification and Classification of a Two-Component System Based on Domain Structures in Bacteria and Differences in Domain Structure between Gram-Positive and Gram-Negative Bacteria. Biosci Biotechnol Biochem **74:**716-720.

11. **Wuichet K, Cantwell BJ, Zhulin IB.** 2010. Evolution and phyletic distribution of two-component signal transduction systems. Current opinion in microbiology **13:**219-225.

12. **Hutchings MI, Hoskisson PA, Chandra G, Buttner MJ.** 2004. Sensing and responding to diverse extracellular signals? Analysis of the sensor kinases and response regulators of *Streptomyces coelicolor A3(2)*. Microbiology **150:**2795-2806.

13. **Yepes A, Rico S, Rodriguez-Garcia A, Santamaria RI, Diaz M.** 2011. Novel two-component systems implied in antibiotic production in *Streptomyces coelicolor*. PLoS One **6:**e19980.

14. **Castro-Melchor M, Charaniya S, Karypis G, Takano E, Hu WS.** 2010. Genome-wide inference of regulatory networks in *Streptomyces coelicolor*. BMC Genomics **11:**578.

15. **Park SS, Yang YH, Song E, Kim EJ, Kim WS, Sohng JK, Lee HC, Liou KK, Kim BG.** 2009. Mass spectrometric screening of transcriptional regulators involved in antibiotic biosynthesis in *Streptomyces coelicolor* A3(2). J Ind Microbiol Biotechnol **36:**1073-1083.

16. **Yang YH, Song E, Willemse J, Park SH, Kim WS, Kim EJ, Lee BR, Kim JN, van Wezel GP, Kim BG.** 2012. A novel function of Streptomyces integration host factor (sIHF) in the control of antibiotic production and

672 sporulation in *Streptomyces coelicolor*. Antonie Van Leeuwenhoek **101:**479-
673 492.
674 17. **Lee PC, Umeyama T, Horinouchi S.** 2002. *afsS i*s a target of AfsR, a
675 transcriptional factor with ATPase activity that globally controls secondary
676 metabolism in *Streptomyces coelicolor* A3(2). Mol Microbiol **43:**1413-1430.
677 18. **Lian W, Jayapal KP, Charaniya S, Mehra S, Glod F, Kyung YS, Sherman**
678 **DH, Hu WS.** 2008. Genome-wide transcriptome analysis reveals that a
679 pleiotropic antibiotic regulator, AfsS, modulates nutritional stress response in
680 *Streptomyces coelicolor* A3(2). BMC Genomics **9:**56.
681 19. **Park U, Suh J, Hong S.** 2000. Genetic analysis of *absR*, anew abs locus of
682 *Streptomyces coelicolor*. Journal of Microbiology and Biotechnology **10:**169-
683 175.
684 20. **Fowler-Goldsworthy K, Gust B, Mouz S, Chandra G, Findlay KC, Chater**
685 **KF.** 2011. The actinobacteria-specific gene *wblA* controls major developmental
686 transitions in *Streptomyces coelicolor* A3(2). Microbiology **157:**1312-1328.
687 21. **Homerova D, Sevcikova J, Kormanec J.** 2003. Characterization of the
688 *Streptomyces coelicolo*r A3(2) *wblE* gene, encoding a homologue of the
689 sporulation transcription factor. Folia microbiologica **48:**489-495.
690 22. **den Hengst CD, Tran NT, Bibb MJ, Chandra G, Leskiw BK, Buttner MJ.**
691 2010. Genes essential for morphological development and antibiotic production
692 in *Streptomyces coelicolor* are targets of BldD during vegetative growth. Mol
693 Microbiol **78:**361-379.
694 23. **Elliot MA, Bibb MJ, Buttner MJ, Leskiw BK.** 2001. BldD is a direct
695 regulator of key developmental genes in *Streptomyces coelicolor A3*(2). Mol
696 Microbiol **40:**257-269.

24. **Datsenko KA, Wanner BL.** 2000. One-step inactivation of chromosomal genes in *Escherichia coli* K-12 using PCR products. Proc Natl Acad Sci U S A **97:**6640-6645.

25. **MacNeil DJ, Gewain KM, Ruby CL, Dezeny G, Gibbons PH, MacNeil T.** 1992. Analysis of *Streptomyces avermitilis* genes required for avermectin biosynthesis utilizing a novel integration vector. Gene **111:**61-68.

26. **Sambrook J, Fritsch E, Maniatis T.** 1989. Molecular cloning: a laboratory manual, 2nd ed. Cold Spring Harbor Laboratory, Cold Spring Harbor, N. Y.

27. **Hopwood DA, Bibb JM, Chater KF, Kieser T, Bruton CJ, Kieser HM, Lydiate DJ, Smith CP, Ward JM, Schrempf H.** 1985. Genetic manipulation of *Streptomyces*: A laboratory manual. John Innes Foundation, Norwich, UK.

28. **Kieser T, Hopwood DA, Bibb JM, Chater KF, Buttner MJ.** 2000. Practical *Streptomyces* genetics. John Innes Foundation, Norwich, UK.

29. **Larson JL, Hershberger CL.** 1986. The minimal replicon of a streptomycete plasmid produces an ultrahigh level of plasmid DNA. Plasmid **15:**199-209.

30. **Sevillano L, Diaz M, Yamaguchi Y, Inouye M, Santamaria RI.** 2012. Identification of the first functional toxin-antitoxin system in *Streptomyces*. PloS one **7:**e32977.

31. **Gust B, Challis GL, Fowler K, Kieser T, Chater KF.** 2003. PCR-targeted *Streptomyces* gene replacement identifies a protein domain needed for biosynthesis of the sesquiterpene soil odor geosmin. Proc Natl Acad Sci U S A **100:**1541-1546.

32. **Gentleman RC, Carey VJ, Bates DM, Bolstad B, Dettling M, Dudoit S, Ellis B, Gautier L, Ge Y, Gentry J, Hornik K, Hothorn T, Huber W, Iacus S, Irizarry R, Leisch F, Li C, Maechler M, Rossini AJ, Sawitzki G, Smith C,**

Smyth G, Tierney L, Yang JY, Zhang J. 2004. Bioconductor: open software development for computational biology and bioinformatics. Genome biology **5:**R80.

33. **R-Core-Team.** 2013. R: a language and environment for statistical computing. R Foundation for Statistical Computing.

34. **Smyth GK, Speed TP.** 2003. Normalization of cDNA microarray data. Methods **31:**265-273.

35. **Laing E, Smith CP.** 2010. RankProdIt: A web-interactive Rank Products analysis tool. BMC Res Notes **3:**221.

36. **Hesketh A, Bucca G, Laing E, Flett F, Hotchkiss G, Smith CP, Chater KF.** 2007. New pleiotropic effects of eliminating a rare tRNA from *Streptomyces coelicolor*, revealed by combined proteomic and transcriptomic analysis of liquid cultures. BMC Genomics **8:**261.

37. **Livak KJ, Schmittgen TD.** 2001. Analysis of relative gene expression data using real-time quantitative PCR and the 2(-Delta Delta C(T)) Method. Methods **25:**402-408.

38. **Bucca G, Laing E, Mersinias V, Allenby N, Hurd D, Holdstock J, Brenner V, Harrison M, Smith CP.** 2009. Development and application of versatile high density microarrays for genome-wide analysis of *Streptomyces coelicolor*: characterization of the HspR regulon. Genome Biol **10:**R5.

39. **Allenby NE, Laing E, Bucca G, Kierzek AM, Smith CP.** 2012. Diverse control of metabolism and other cellular processes in *Streptomyces coelicolor* by the PhoP transcription factor: genome-wide identification of in vivo targets. Nucleic acids research **40:**9543-9556.

40. **Pérez J, Muñoz-Dorado J, Braña AF, Shimkets LJ, Sevillano L, Santamaría RI.** 2011. *Myxococcus xanthus* induces actinorhodin overproduction and aerial mycelium formation by *Streptomyces coelicolor*. Microb Biotechnol **4:**175-183.

41. **Lewis RA, Laing E, Allenby N, Bucca G, Brenner V, Harrison M, Kierzek AM, Smith CP.** 2010. Metabolic and evolutionary insights into the closely-related species *Streptomyces coelicolor* and *Streptomyces lividans* deduced from high-resolution comparative genomic hybridization. BMC genomics **11:**682.

42. **Zhang YX, Denoya CD, Skinner DD, Fedechko RW, McArthur HA, Morgenstern MR, Davies RA, Lobo S, Reynolds KA, Hutchinson CR.** 1999. Genes encoding acyl-CoA dehydrogenase (AcdH) homologues from *Streptomyces coelicolor* and *Streptomyces avermitilis* provide insights into the metabolism of small branched-chain fatty acids and macrolide antibiotic production. Microbiology **145 (Pt 9):**2323-2334.

43. **Capstick DS, Jomaa A, Hanke C, Ortega J, Elliot MA.** 2011. Dual amyloid domains promote differential functioning of the chaplin proteins during *Streptomyces* aerial morphogenesis. Proceedings of the National Academy of Sciences of the United States of America **108:**9821-9826.

44. **Uguru GC, Stephens KE, Stead JA, Towle JE, Baumberg S, McDowall KJ.** 2005. Transcriptional activation of the pathway-specific regulator of the actinorhodin biosynthetic genes in *Streptomyces coelicolor*. Mol Microbiol **58:**131-150.

45. **Gao C, Hindra, Mulder D, Yin C, Elliot MA.** 2012. Crp is a global regulator of antibiotic production in *Streptomyces*. MBio **3**.

769 46. **Sola-Landa A, Moura RS, Martin JF.** 2003. The two-component PhoR-PhoP
770 system controls both primary metabolism and secondary metabolite biosynthesis
771 in *Streptomyces lividans*. Proc Natl Acad Sci U S A **100:**6133-6138.
772 47. **Lu Y, Wang W, Shu D, Zhang W, Chen L, Qin Z, Yang S, Jiang W.** 2007.
773 Characterization of a novel two-component regulatory system involved in the
774 regulation of both actinorhodin and a type I polyketide in *Streptomyces*
775 *coelicolor*. Appl Microbiol Biotechnol **77:**625-635.
776 48. **Guerra SM, Rodriguez-Garcia A, Santos-Aberturas J, Vicente CM, Payero**
777 **TD, Martin JF, Aparicio JF.** 2012. LAL regulators SCO0877 and SCO7173 as
778 pleiotropic modulators of phosphate starvation response and actinorhodin
779 biosynthesis in *Streptomyces coelicolor*. PloS one **7:**e31475.
780 49. **Feng WH, Mao XM, Liu ZH, Li YQ.** 2011. The ECF sigma factor SigT
781 regulates actinorhodin production in response to nitrogen stress in *Streptomyces*
782 *coelicolor*. Applied microbiology and biotechnology **92:**1009-1021.
783 50. **McKenzie NL, Nodwell JR.** 2007. Phosphorylated AbsA2 negatively regulates
784 antibiotic production in *Streptomyces coelicolor* through interactions with
785 pathway-specific regulatory gene promoters. J Bacteriol **189:**5284-5292.
786 51. **Wang R, Mast Y, Wang J, Zhang W, Zhao G, Wohlleben W, Lu Y, Jiang**
787 **W.** 2013. Identification of two-component system AfsQ1/Q2 regulon and its
788 cross-regulation with GlnR in *Streptomyces coelicolor*. Molecular microbiology
789 **87:**30-48.
790 52. **Yu Z, Zhu H, Dang F, Zhang W, Qin Z, Yang S, Tan H, Lu Y, Jiang W.**
791 2012. Differential regulation of antibiotic biosynthesis by DraR-K, a novel two-
792 component system in *Streptomyces coelicolor*. Molecular microbiology **85:**535-
793 556.

53. **Higo A, Hara H, Horinouchi S, Ohnishi Y.** 2012. Genome-wide Distribution of AdpA, a Global Regulator for Secondary Metabolism and Morphological Differentiation in *Streptomyces*, Revealed the Extent and Complexity of the AdpA Regulatory Network. DNA Res **19:**259-274.

54. **Wang W, Shu D, Chen L, Jiang W, Lu Y.** 2009. Cross-talk between an orphan response regulator and a noncognate histidine kinase in *Streptomyces coelicolor*. FEMS Microbiol Lett **294:**150-156.

804 **TABLES**

805 TABLE 1 - Selected genes significantly down-regulated in the Δ*abrC3* mutant relative

806 to parent strain, M145 (p-value< 0.005 and/or pfp*<0.15)

SCO/name	Function	p-value	pfp	Fold change	Time (hours)
5071	Hydroxylacyl-CoA dehydrogenase	0	0.002	-1.77	48
5072	Hydroxylacyl-CoA dehydrogenase	0	0	-2.13	48
5073	Putative oxidoreductase	0	0	-2.09	48
5074	Putative dehydratase	0	0	-3.25	48
5075/ORF4	Putative oxidoreductase	0	0	-2.23	48
5077/actVA2	Hypothetical protein	0	0.001	-1.99	48
5078/actVA3	Hypothetical protein	0	0	-2.28	48
5079/actVA4	Conserved hypothetical protein	0	0	-2.28	48
5080/actVA5	Putative hydrolase	0	0	-2.25	48
5081/actVA6	Hypothetical protein	0	0	-2.59	48
5085/actII-ORF4	Actinorhodin cluster activator protein	0	0	-2.85	48
5086/actIII	Ketoacyl reductase	0	0	-2.80	48
5087/actIORF1	Actinorhodin polyketide beta-ketoacyl synthase alpha subunit	0	0.008	-1.83	48
5088/actIORF2	Actinorhodin polyketide beta-ketoacyl synthase beta subunit	0	0.003	-1.92	48
5089/actIORF3	Actinorhodin polyketide synthase acyl carrier protein	0	0	-3.11	48
5090/actVII	Actinorhodin polyketide synthase bifunctional cyclase/dehydratase	0.0002	0.060	-1.63	48
0045	Hypothetical protein	0.0005	0.127	-1.23	48
0682	Hypothetical protein SCF15.03c	0.0001	0.053	-1.25	48
0736	Putative secreted protein	0	0.019	-1.45	60
1480/sIHF	*Streptomyces* Integration Host Factor	0.0003	0.090	-1.28	48
1550	Putative small membrane protein	0.0002	0.070	-1.35	36
1839	Putative transcriptional regulator	0.0005	0.120	-1.40	36
2113/bfr	Putative bacterioferritin	0.0001	0.050	-1.24	48
2779/acdH	Acyl-CoA dehydrogenase	0.0006	0.145	-1.27	36
3218	Putative small conserved hypothetical protein	0	0.018	-1.39	36
3327	Hypothetical protein	0.0002	0.051	-1.41	60
3328/bdtA	Hypothetical protein	0.0002	0.055	-1.47	60
4425/afsS	Sigma-like protein	0	0.001	-1.83	48
5240/wblE	Hypothetical protein	0.0007	0.158	-1.36	48
5915	Fatty acid desaturase	0.0003	0.081	-1.39	36
6205	Putative threonine dehydrogenase	0.0007	0.158	-1.43	48
6992/*absR1*	Regulatory protein	0.0001	0.056	-1.57	60

807 * *pfp*: *p*robability of *f*alse *p*rediction

808

809

TABLE 2 - Selected genes up-regulated in the Δ*abrC3* mutant relative to the parent strain, M145 (p-value< 0.005 and/or pfp*<0.15)

SCO/name	Function	p-value	Pfp	Fold change	Time
1800/chpE	Putative small secreted protein	0.0001	0.145	1.12	48
2605	Hypothetical protein SCC88.16	0.0002	0.140	1.36	36
4187	Putative membrane protein	0	0.040	1.52	36
4709/rplP	50S ribosomal protein L16	0.0001	0.119	1.16	36
6329	Hypothetical protein SC10H5.05	0.0001	0.115	1.38	60
6809	Putative integral membrane transport protein	0.0001	0.124	1.41	60
7665	Hypothetical protein	0.0002	0.131	1.07	36
7801	Putative membrane protein	0.0002	0.131	1.39	60

***** *pfp*: *p*robability of *f*alse *p*rediction

TABLE 3. qRT-PCR validation of five differentially expressed genes identified from microarray data. Linear regression fit analysis was applied and correlation coefficient used to validate the data ($y = 1.60x – 0,09$; $R^2 = 0.93$)

SCO/name	Function	Expression ratios (fold change)[a]	
		Microarray	RT-qPCR
2779/acdH	Acyl-Coa dehydrogenase	-1.27	-2.13
4425/afsS	Sigma like protein	-1.83	-3.06
4597/abrC2	Sensor kinase	-1.085	-1.12
4598/abrC1	Sensor Kinase	-1.04	-1.08
5085/actII-ORF4	ACT cluster activation protein	-2.85	-3.90
6992/AbsR1	Regulatory protein	-1.57	-3.65
4709/rplP	50S ribosomal protein L16	1.16	2.11

[a] parent strain M145 *versus* Δ*abrC3*

821 TABLE 4. AbrC3 ChIP-chip targets selected by their high enrichment ratio

Regulated gene[a]	Enrichment ratio[b]	Predicted function of regulated gene	Time[c]	Predicted binding site sequence[d]
SCO0167	2.45	Conserved hypothetical protein SCJ1.16c	36	354 GAAGGGGGCG 363
SCO0951	2.22	Putative transport system permease protein	36	-329 GGTCGCCTTC -318
SCO1391	5.44	*crr* ,phosphoenolpyruvate-protein phosphotransferase	48	1113 GAAGGCGGCG 1122
SCO3020	4.22	Putative integral membrane protein	48	Not found
SCO3263	2.60	Conserved hypothetical protein	36	-240 GTTCGCCTTC -231
SCO3334	5.70	*trpS*, tryptophanyl tRNA synthetase	48	-387 GGCCGCGTTC -378
SCO3590	2.54	*vanR,* putative TCS response regulator	36	Not found
SCO3992	2.45	Hypothetical protein	36	Not found
SCO4075	6.32	*ragA,* ABC transport protein, ATP-binding subunit	48	Not found
SCO4123	5.02	Putative TCS response regulator	48	-674 GAACGCGACC -665
SCO4596	**2.24**	***abrC3,* TCS response regulator**	**60**	**-137 CTTCCCGTTC -128**
SCO4630	2.78	Hypothetical protein	36	Not found
SCO5085	**2.23**	***actII-ORF4,* ACT cluster activator protein**	**36**	**72 GAAGGCGACC 81**
SCO5236	2.86	*nagB,* putative glucosamine phosphate isomerase	48	-213 GGTCGCGTTC -204
SCO5330	3.26	Hypothetical protein SC6G9.03c	36	-975 GAAGGGGGCG -966
SCO5332	2.21	Hypothetical protein	36	1134 CTTCGCCTTC 1143
SCO5632	2.36	Hypothetical protein SC6A9.3	36	-1261 GAACGGGACG -1252
SCO5638	2.76	Integral membrane protein	36	X
SCO5691	2.24	Putative secreted sugar hydrolase	48	-777 GAACGCGGCG -768
SCO5729	2.33	Conserved hypothetical protein SC3C3.15c	36	Not found
SCO5912	4.30	Probable secreted protease	48	-54 CTCCCCCTTC -45
SCO5966	2.24	Putative oxidase	48	-803 GAAGGCGGAC -794
SCO6273	2.18	*cpkC,* putative type I polyketide synthase	48	3138 CGCCCCGTTC 3147
SCO6732	2.29	Putative fatty acid oxidative multifunctional enzyme	36	1140 GAAGGCGGCC 1149
SCO6820	2.94	Putative oxidoreductase	48	-519 GAACGCGGCC -510
SCO6941	2.55	*cvnC8,* hypothetical protein SC1G8.13c	36	-306 GGCCGCCTTC -297
SCO6951	2.55	Conserved hypothetical protein	36	-411 CGCCGCGTTC -402
SCO6992	**2.78**	***absR1,* regulatory protein**	**48**	**-321 GAAGGGGACG -312**
SCO7077	2.24	Putative integral membrane protein	36	-294 GAAGGCGGCG -285
SCO7545	2.45	Putative ABC-transport protein, ATP-binding component	48	-369 GGCCGCGTTC -360

822 [a] Putative AbrC3-target genes indicated by the ChIP-chip analysis.

823 [b] AbrC3-DNA interaction affinity.

824 [c] Time of the ChIP-chip assay at which the shown enrichment ratio has been found.

825 [d] Consensus Binding site sequence: 5'-GAASGSGRMS-3'; Numbers indicate the

826 position of the sequence related to the start codon of the corresponding gene.

827 The genes that have also shown differential transcription profile are in bold.

828

829 TABLE 5. AbrC3 overlapping targets in ChIP-chip and transcriptome analyses

SCO	Enrichment ratio[a]	Predicted function of regulated gene	Time[b]	Predicted binding site sequence[c]
SCO0736	1.50	Putative secreted protein	36	-53 GAAGGCGACC -44
SCO2113	1.59	*bfr*, putative bacterioferritin	48	-26 GTTCCCGTTC -17
SCO3328	1.48	*bdtA,* hypothetical protein	48	-46 GAAGGGGAAG -37
SCO4596	2.24	*abrC3,* TCS response regulator	60	-137 CTTCCCGTTC -128
SCO4709	**1.89**	***rplP*, 50S ribosomal protein L16**	**36**	**Not found**
SCO5085	2.23	*actII-ORF4,* ACT cluster activator protein	36	72 GAAGGCGACC 81
SCO6809	**1.77**	**Putative integral membrane transport protein**	**48**	**-112 GAAGGCGGAC -103**
SCO6992	2.78	*absR1,* regulatory protein	48	-321 GAAGGGGACG -312

830 [a] AbrC3-DNA interaction affinity by ChIP-chip

831 [b] Time of the ChIP-chip assay at which the shown enrichment ratio has been found.

832 [c] Consensus Binding site sequence: 5'-GAASGSGRMS-3'; Numbers indicate the

833 position of the sequence related to the start codon of the corresponding gene

834 The genes in bold are up-regulated. The other genes of the table are down-regulated

835

836

837

838 **FIGURE' LEGENDS**

839

840 Figure 1: Phenotypic study of the mutants, complementation and overexpression

841 A) Production of the antibiotics ACT (72 h), CDA (bioassay against *B. subtilis* at 48 h),

842 and RED (48 h), by the parent strain (M145) and the mutants Δ*abrC1/2/3* and Δ*abrC3*

843 and their morphological differentiation (MD) on NA medium.

844 B) Complementation of ACT production by integration of plasmid pSETabrC3 in the

845 mutant strain Δ*abrC3* in liquid medium NB (ACT liquid), and ACT (72 h), RED (48 h)

846 and their morphological differentiation (MD) on solid NA medium.

847

848 Figure 2: Overexpression of AbrC3 in *S. coelicolor* and *S. lividans.*

849 ACT production of *S. coelicolor* M145 (left) and *S. lividans* 66 (right) transformed with

850 low copy number plasmid pHJL401 (control) and its derivative pHJLabrC3 in NB

851 medium at 5 days. Error bars correspond to three independent experiments. In the

852 bottom part a photograph of the corresponding supernatants.

853

854 Figure 3: EMSA of AbrC3 protein with ChIP-chip selected promoters

855 EMSA of the AbrC3 protein with different concentration of the protein; A) *actII-*

856 *ORF4p*; B) *abrC3p*; C) *SCO0736p;* D) *absR1p* (*SCO6992);* E) *SCO2113p;* F) *bdtAp*

857 *(SCO3328);* G) *SCO4709p;* H) *SCO6809p.* S: specific competition control (adding the

858 corresponding unlabelled specific probe); N: non-specific competitor DNA (100-fold

859 molar excess of sheared sperm salmon DNA), BSA: protein specific control (4 µM of

860 BSA protein).

861

Figure 4: Identification of a putative AbrC3-binding sequence in different genes

A) Consensus sequence identified with the Regulatory Sequence Analysis Tool consensus alignment of putative promoters* (up to - 400 bp upstream sequences plus +100 from the translational start point) of genes identified by ChIP-chip and EMSAs. B) EMSAs of different fragments of the *actII-ORF4* promoter* region with 4 μM AbrC3 (top panel, a scheme of the amplified fragment location in the promoter*). C) EMSA of AbrC3 protein with *actII-ORF4* fragment 4 promoter* with different concentration of the protein; S: specific competition control (adding 100-fold molar excess of unlabelled specific probe); N: non-specific competitor DNA (adding 100-fold excess of sheared sperm salmon DNA), BSA: specific control-2 (adding 4 μM of BSA protein).

Figure 5: Location of regulatory protein binding sites in the *actII-ORF4* promoter* region

Location of the binding sequences described in the literature for the proteins AtrA, DraR, and AfsQ1 in the *actII-ORF4* promoter* and the position of the deduced target sequence for AbrC3 identified in this work

Figure 6. Scheme of the AbrC3 regulon of *S. coelicolor*.

Schematic model of the pleiotropic regulatory role of AbrC3 in primary and secondary metabolism, morphological differentiation, and the putative gene network governed by AbrC3. → positive control (green); —♦ negative control (red); —— direct control (solid line); − − − indirect control (dashed line). (1) data from Wang *et al.,* 2013.

Figure 1

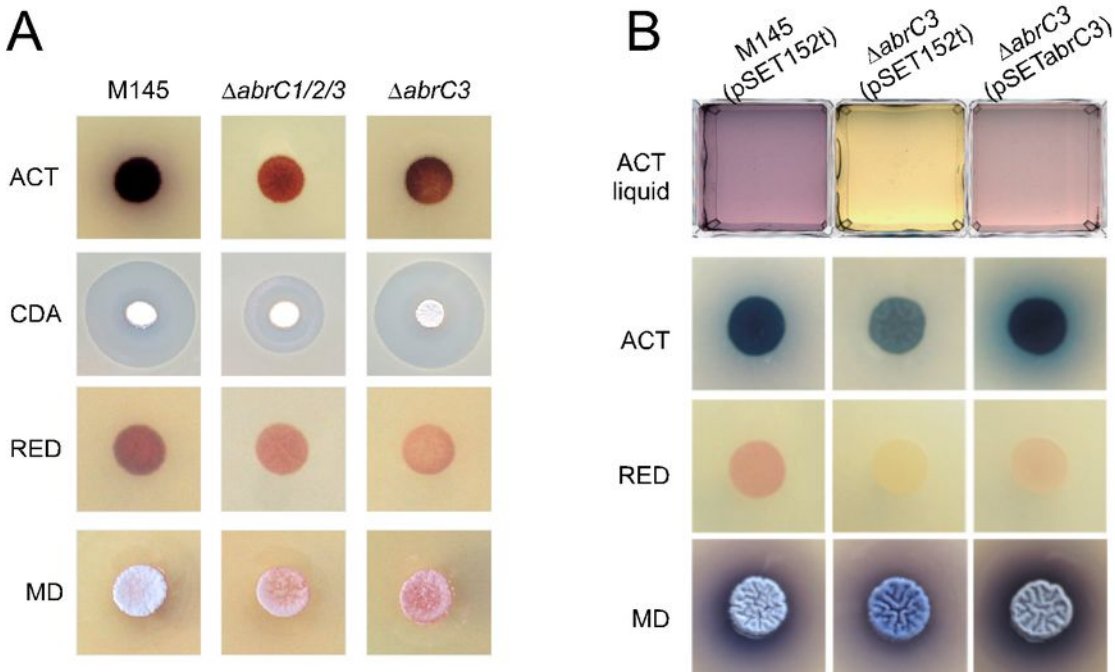
A
M145
ΔabrC1/2/3
ΔabrC3
ACT
CDA
RED
MD
B
M145 (pSET152t)
ΔabrC3 (pSET152t)
ΔabrC3 (pSETabrC3)
ACT liquid
ACT
RED
MD

Figure 2

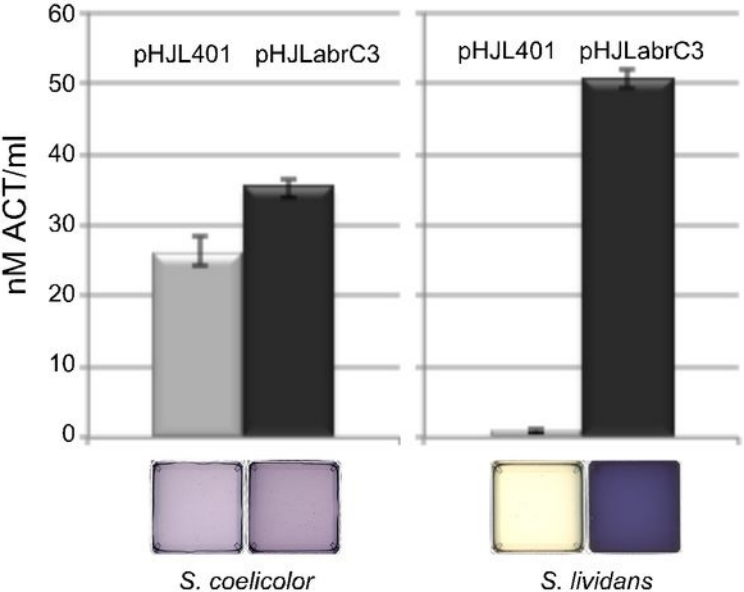
60
50
40
30
20
10
0
nM ACT/ml
pHJL401
pHJLabrC3
pHJL401
pHJLabrC3
S. coelicolor
S. lividans

Figure 3

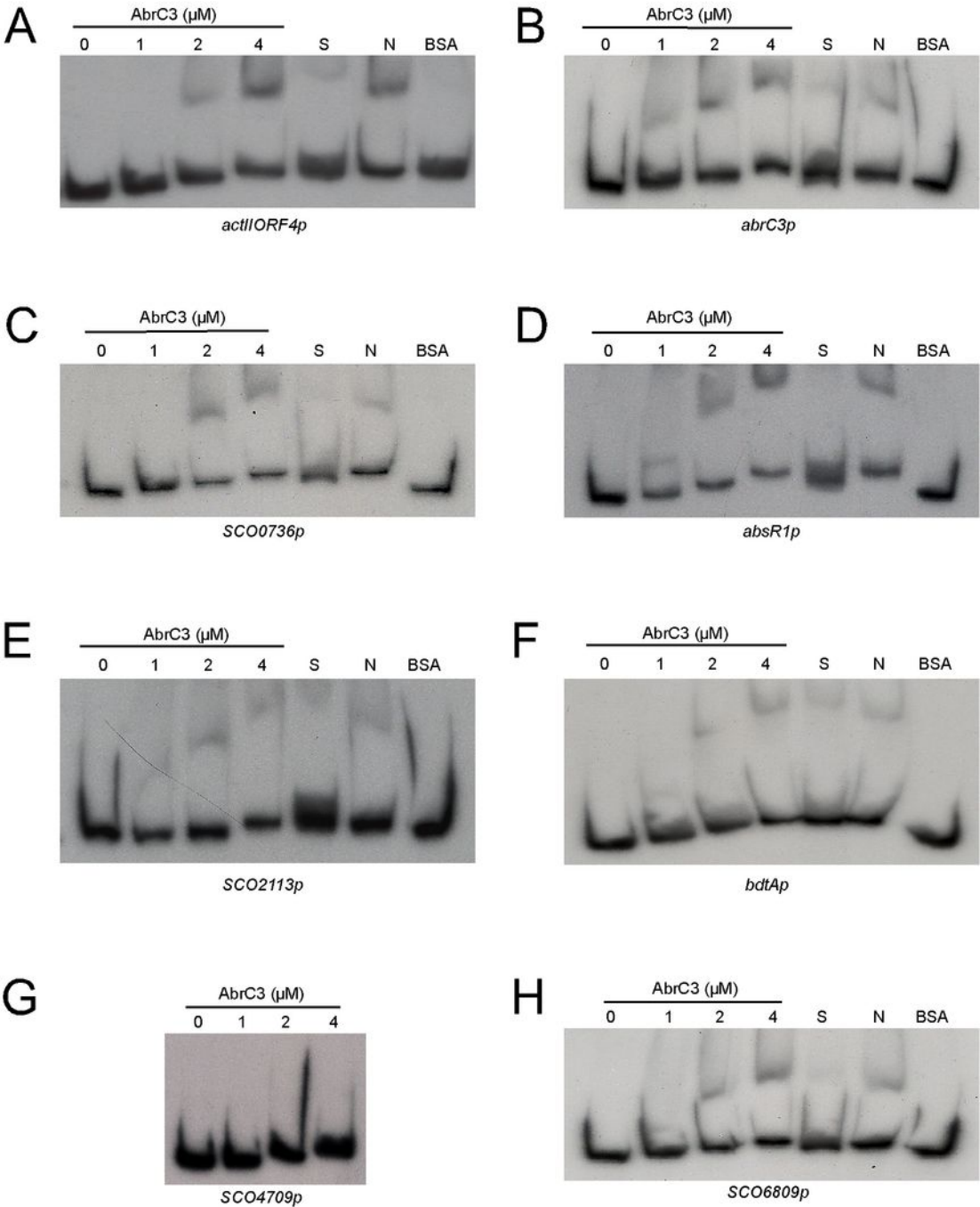
A
AbrC3 (μM)
0 1 2 4 S N BSA
actIIORF4p
B
AbrC3 (μM)
0 1 2 4 S N BSA
abrC3p
C
AbrC3 (μM)
0 1 2 4 S N BSA
SCO0736p
D
AbrC3 (μM)
0 1 2 4 S N BSA
absR1p
E
AbrC3 (μM)
0 1 2 4 S N BSA
SCO2113p
F
AbrC3 (μM)
0 1 2 4 S N BSA
bdtAp
G
AbrC3 (μM)
0 1 2 4
SCO4709p
H
AbrC3 (μM)
0 1 2 4 S N BSA
SCO6809p

Figure 4

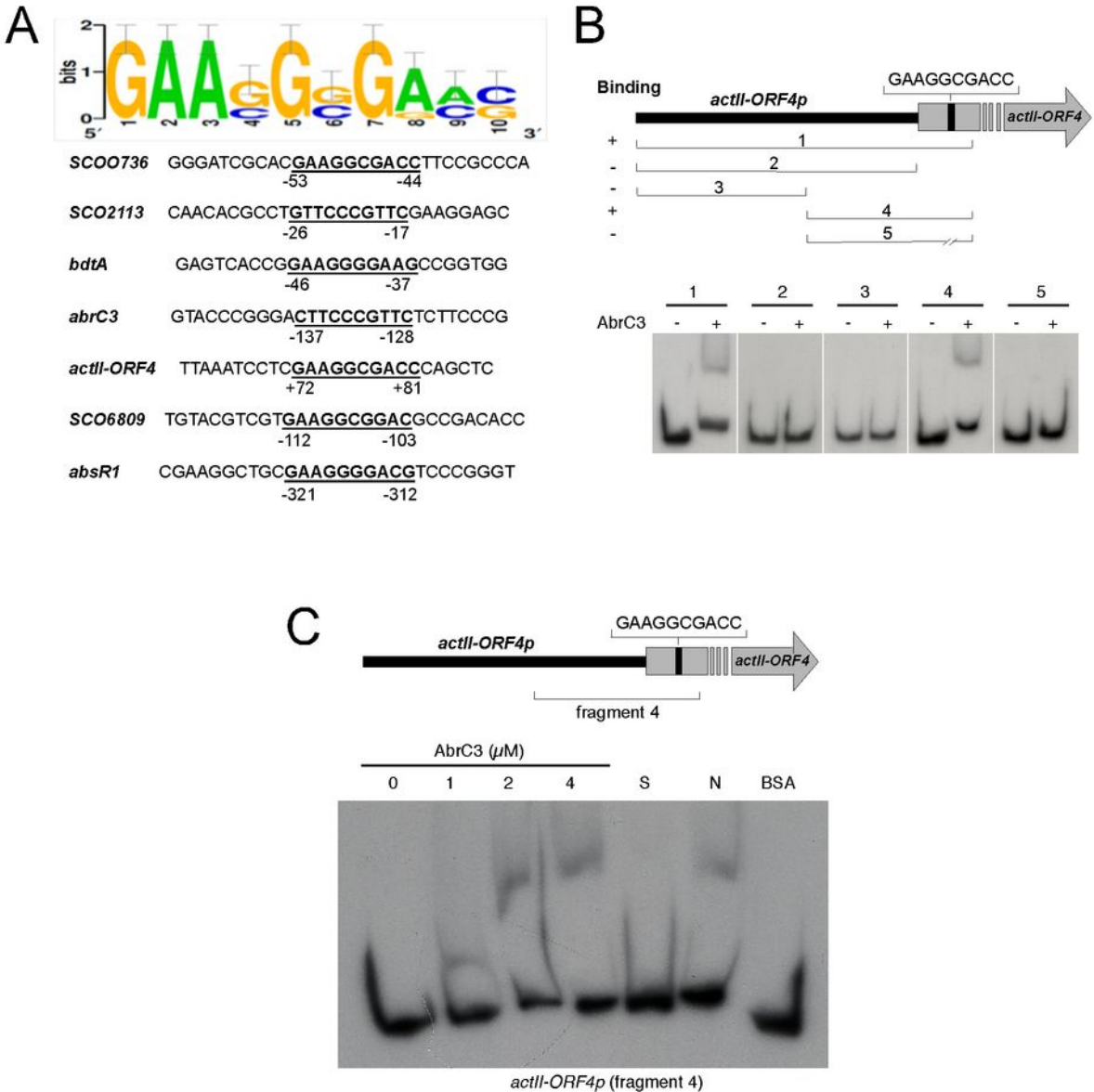
A
bits
5′
3′
SCO0736 GGGATCGCACGAAGGCGACCTTCCGCCCA
-53 -44
SCO2113 CAACACGCCTGTTCCCGTTCGAAGGAGC
-26 -17
bdtA GAGTCACCGGAAGGGGAAGCCGGTGG
-46 -37
abrC3 GTACCCGGGACTTCCCGTTCTCTTCCCG
-137 -128
actII-ORF4 TTAAATCCTCGAAGGCGACCCAGCTC
+72 +81
SCO6809 TGTACGTCGTGAAGGCGGACGCCGACACC
-112 -103
absR1 CGAAGGCTGCGAAGGGGACGTCCCGGGT
-321 -312
B
Binding
actII-ORF4p
GAAGGCGACC
actII-ORF4
1
2
3
4
5
AbrC3
C
actII-ORF4p
GAAGGCGACC
actII-ORF4
fragment 4
AbrC3 (μM)
0 1 2 4 S N BSA
actII-ORF4p (fragment 4)

Figure 5.

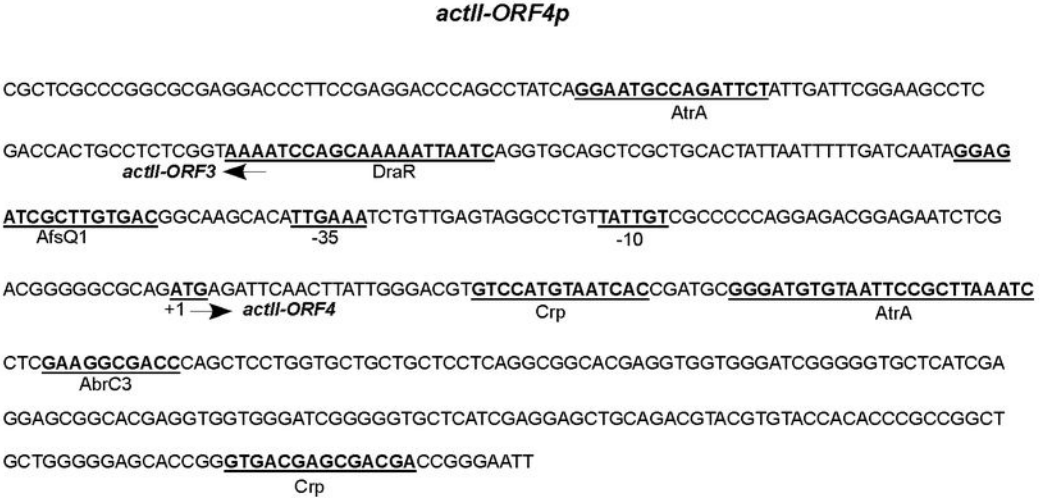
actII-ORF4p
CGCTCGCCCGGCGCGAGGACCCTTCCGAGGACCCAGCCTATCAGGAATGCCAGATTCTATTGATTCGGAAGCCTC
AtrA
GACCACTGCCTCTCGGTAAAATCCAGCAAAAATTAATCAGGTGCAGCTCGCTGCACTATTAATTTTTGATCAATAGGAG
actII-ORF3
DraR
ATCGCTTGTGACGGCAAGCACATTGAAATCTGTTGAGTAGGCCTGTTATTGTCGCCCCCAGGAGACGGAGAATCTCG
AfsQ1
-35
-10
ACGGGGGCGCAGATGAGATTCAACTTATTGGGACGTGTCCATGTAATCACCGATGCGGGATGTGTAATTCCGCTTAAATC
+1
actII-ORF4
Crp
AtrA
CTCGAAGGCGACCCAGCTCCTGGTGCTGCTGCTCCTCAGGCGGCACGAGGTGGTGGGATCGGGGGTGCTCATCGA
AbrC3
GGAGCGGCACGAGGTGGTGGGATCGGGGGTGCTCATCGAGGAGCTGCAGACGTACGTGTACCACACCCGCCGGCT
GCTGGGGGAGCACCGGGTGACGAGCGACGACCGGGAATT
Crp

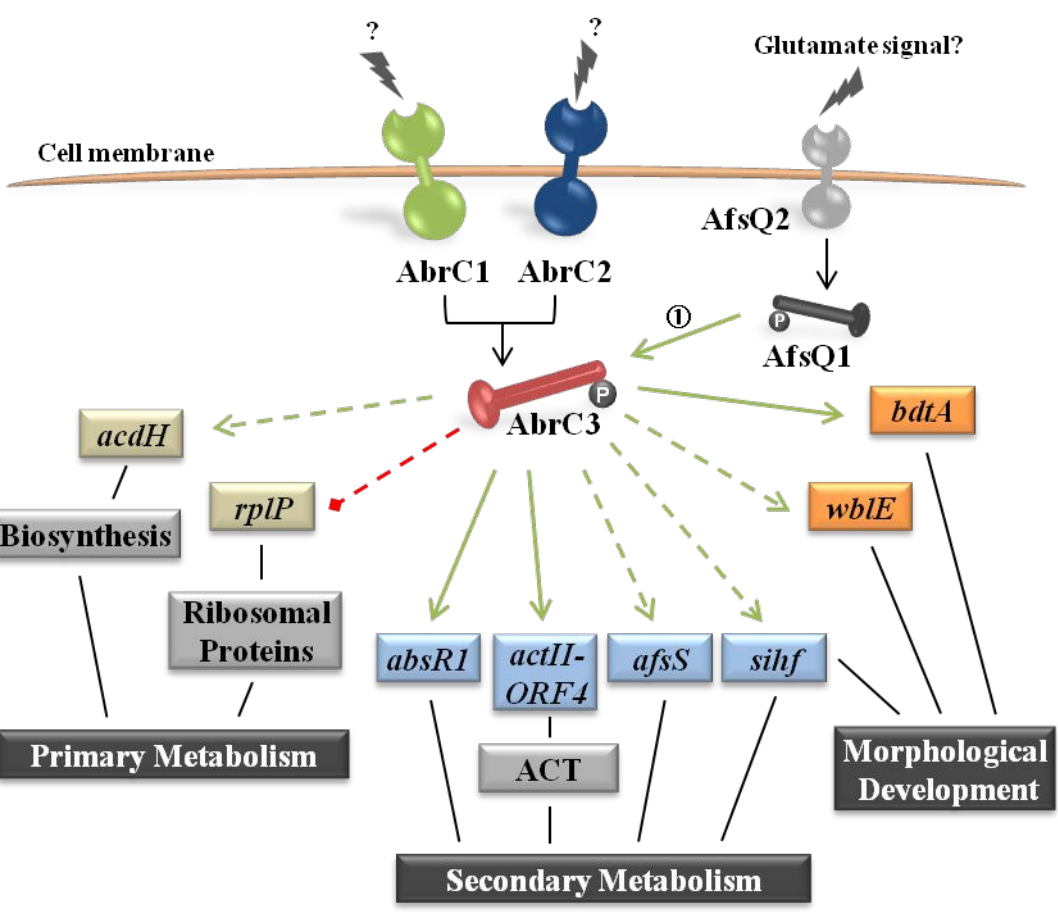
?
?
Glutamate signal?
Cell membrane
AfsQ2
AbrC1
AbrC2
①
AfsQ1
P
AbrC3
P
bdtA
acdH
rplP
wblE
Biosynthesis
Ribosomal Proteins
absR1
actII-ORF4
afsS
sihf
Primary Metabolism
ACT
Morphological Development
Secondary Metabolism